Performance of synergistic ultrasonic degradation of dye wastewater by nano zinc oxide with different morphologies

Chunying Bai*

College of Mining and Chemical Engineering, Hulunbuir University, Hulunbeier, China.

***Corresponding author**: bcy137@126.com

Abstract:

By nthesizing nano zinc oxide with different morphologies, such as spherical, snowflake like, and starfish like, and utilizing its unique physical and chemical properties, combined with the cavitation effect of ultrasound, it is expected to achieve effective degradation of dye wastewater. In the comparative experiment of using nano zinc oxide, ultrasound, ultrasound+nano zinc oxide to treat methyl orange solution, the research method showed the most significant change in absorbance. At 20 minutes, the absorbance decreased by 50.07%, and after 2 hours, the absorbance decreased to 0.012A. The degradation rate of methyl orange solution was significantly improved by the research method, reaching 99.23% after 2 hours, which is higher than the degradation rate of 76.68% using only nano zinc oxide and 51.52% using only ultrasound treatment. The first-order kinetic curve k value of the research method for treating methyl orange solution was 0.002 min^{-1}, with an R^2 of 0.995. In the treatment experiment of three types of nano zinc oxide, the degradation rate of starfish shaped nano zinc oxide was the highest, reaching the maximum value of 99.56% after 2 hours, which is better than the treatment effect of spherical and snowflake shaped nano zinc oxide.

1. Introduction

The rapid development of industry has made dye wastewater one of the serious environmental pollution problems. The organic dyes in dye wastewater not only harm the environment, but also pose a serious threat to human health [1]. Therefore, seeking effective methods for treating dye wastewater has become an urgent problem to be solved. In recent years, nanomaterials have attracted much attention due to their unique physical and chemical properties, and have been widely used in fields such as photocatalysis, photoelectric conversion, and photothermal conversion [2]. Nano zinc oxide (N-ZnO) is a novel nanomaterial with high activity, wide absorption spectrum, and high stability [3]. The morphology and size of N-ZnO have a significant impact on its physical and chemical properties. Different morphologies of N-ZnO have different specific surface areas and crystal structures, which affect their photocatalytic performance. In addition, N-ZnO also has good photosta-

bility and chemical stability, which can effectively degrade organic pollutants [4]. Ultrasonic technology is an efficient and environmentally friendly method for wastewater treatment. Ultrasound can generate strong cavitation effects, leading to free radical reactions and chemical degradation [5, 6]. In view of this, this study will synthesize N-ZnO with different morphologies and utilize its unique physical and chemical properties to synergize the cavitation effect of ultrasound, aiming to achieve the degradation of dye wastewater. This study has the following significance: Firstly, N-ZnO is a material with high catalytic activity, which can effectively degrade organic pollutants. By studying the degradation performance of N-ZnO with different morphologies, a deeper understanding of its degradation mechanism and laws can be obtained, providing theoretical support for optimizing degradation processes. If efficient degradation of dye wastewater can be achieved, it will help solve water pollution problems and improve environmental quality. Finally, this study can provide new research
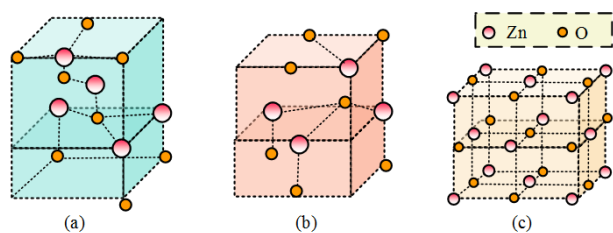
Figure 1. Nano zinc oxide structure
Note: (a), (b), and (c) respectively show the sphalerite, hexagonal wurtzite, and rock salt structures of N-ZnO.

Figure 2. Graphical representation of ultrasonic cavitation effect.

directions for the development of nanomaterials and environmental protection.

2. Principles of experimental materials

2.1 Structure and mechanism of N-ZnO materials

Zinc oxide is an inorganic compound with the chemical formula ZnO, which is an oxide of zinc. It is insoluble in water and ethanol, but can be soluble in acids, sodium hydroxide aqueous solutions, and ammonium chloride. ZnO has a large bandgap and exciton binding energy, high transparency, and excellent room temperature luminescence performance. It has been applied in products such as liquid crystal displays, thin film transistors, and light-emitting diodes in the semiconductor field [7]. N-ZnO is a novel inorganic material with particle sizes ranging from 1 to 100 nanometers. This material has specific physical and chemical properties. Compared with traditional ZnO, its specific surface area increases sharply and its surface molecular activity is high. N-ZnO has excellent photocatalytic performance and has a wide range of applications in the field of optoelectronics [8]. In addition, it also has characteristics such as high transparency and dispersion, and can be used as a catalyst, optoelectronic material, antibacterial agent, etc. [9]. In the field of environmental protection, N-ZnO can be used for photocatalytic purification of air and water quality, decomposition of organic and inorganic pollutants. There are three common crystal structures of N-ZnO: sphalerite type, hexagonal columnar type, and hexagonal ZnO, as shown in Figure 1.

In Figure 1, the sphalerite structure is the most common crystal structure of N-ZnO. In the structure of sphalerite, each zinc ion is surrounded by eight oxygen ions, and each oxygen ion is also surrounded by eight zinc ions. This structure has good optoelectronic performance and is an important application form of N-ZnO in optoelectronic devices. The hexagonal wurtzite structure is another common crystal structure of N-ZnO, which is a hexagonal crystal system structure with high crystal symmetry. In the hexagonal wurtzite structure, each zinc ion is surrounded by six oxygen ions, and each oxygen ion is surrounded by four zinc ions. This structure has excellent optical performance and is often used in fields such as optical devices and photocatalysis. The rock salt type structure is another crystal structure of N-ZnO. The symmetry of the rock salt structure is relatively low, with each zinc ion surrounded by four oxygen ions and each oxygen ion surrounded by two zinc ions. This
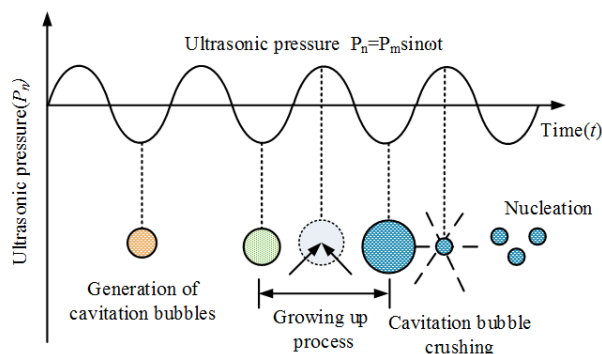
structure can exhibit excellent physical and chemical properties under specific conditions. N-ZnO has many unique physical and chemical properties, making it widely used in multiple fields [10–12]. In addition to its well-known photocatalytic performance, which can convert light energy into electrical energy, N-ZnO also has other characteristics. One of them is that under the action of force, N-ZnO can induce charges on the material surface, a phenomenon known as piezoelectricity [13]. This is mainly attributed to the charge transfer effect in its crystal structure. When external forces act on N-ZnO, it will cause the charge in the crystal structure to redistribute, thereby inducing charges on the material surface. This characteristic makes it have potential applications in fields such as sound wave detection, vibration energy collection, and pressure sensing [14]. In view of this, it is reasonable to apply N-ZnO to degrade dye wastewater.

2.2 The degradation mechanism of ultrasound

Ultrasonic catalysis technology is a method of using ultrasound to excite catalysts, with the aim of catalyzing the conversion of molecules in reactants to improve reaction rate and product yield. This technology is mainly based on the phenomenon of acoustic cavitation, which is the formation of cavitation bubbles at the bubbles in water or on the surface of catalysts by ultrasound. When cavitation bubbles rupture, local high temperature (5000 K), high pressure (100 MPa), and sonoluminescence phenomena are formed, promoting the generation of strong oxidizing monomers such as hydroxyl radicals. Pollutants can be removed through pyrolysis reactions, free radical oxidation, photocatalytic effects, shock wave and micro jet effects, mechanical shear effects, ultrasonic flocculation effects, and other pathways [15]. The mechanism of ultrasonic catalytic degradation of organic compounds mainly comes from the phenomenon of acoustic cavitation, and its reaction process is Figure 2.

Acoustic cavitation refers to the generation of tiny bubble nuclei by ultrasound in liquids. These bubble nuclei are excited by ultrasound, exhibiting a series of dynamic processes such as oscillation, growth, contraction, and collapse of the bubble nuclei. During the negative pressure half cycle of sound waves, when a sufficiently strong ultrasound passes through a liquid, if the amplitude of the sound pressure exceeds the static pressure inside the liquid, the small bubbles

Table 1. Experimental equipment used.

Experimental instruments	Model	Manufacturer
Scanning electron microscope (SEM)	Phenom ProX	Phenom, Netherlands
Ultraviolet-visible spectrophotometer	UH4150	Hitachi, Japan
Power amplifier	AG1024	T&G Power Conversion,inc
Small fan	FSJ-208	Tiantian Special Selling Factory
Ultrasonic cleaning machine	BG-03C	China Bangjie Electronics
X-ray electron spectroscopy analyzer	ESCALAB 250Xi	ThermoFisher Scientific, USA

(cavitation nuclei) present in the liquid will rapidly increase. In the successive positive pressure periods of sound waves, bubbles undergo adiabatic compression and collapse, generating extremely brief strong pressure pulses at the moment of collapse. High temperatures above 5000 K are generated in the middle of the bubbles. The local pressure is above 5×107 Pa, and the temperature at the interface between bubbles and water can also reach 2000 K. Due to the existence of local high temperature and high pressure for only a few microseconds, the temperature change rate is as high as 109 K/s, accompanied by strong shock waves and jets with speeds of up to 400 km/h. This creates an extreme physical and chemical environment for the degradation of organic matter. During the process of acoustic cavitation, organic pollutants in the liquid will be adsorbed and decomposed by cavitation bubbles [16]. Meanwhile, the collapse of cavitation bubbles will release strong oxidizing substances such as hydroxyl radicals. These substances can undergo oxidation-reduction reactions with organic pollutants, causing them to decompose into small molecules or harmless substances. In addition, the mechanical shear effect and shock wave and micro jet effect of ultrasound can also physically break and disperse organic matter, promoting its degradation. It should be noted that in the process of ultrasonic catalytic degradation of organic compounds, factors such as the frequency, intensity, duration of action of ultrasonic waves, as well as the type and concentration of catalysts, can affect the degradation effect. Therefore, in practical applications, it is necessary to optimize and control various factors according to specific situations.

3. Preparation and analysis of experimental materials

3.1 Materials and instruments used in experiments

Table 1 shows the experimental equipment used to prepare N-ZnO with different morphologies using hydrothermal method.

Table 1 provides a detailed record of the various instruments used in the experiment, their models, and manufacturers. These instruments include rotary evaporator, UV visible spectrometer, X-ray powder diffractometer (X-rPD), SEM, etc. The UV visible spectrometer is used to detect the absorption spectrum of samples. X-rPD is used to determine the crystal structure of samples. SEM is used to observe the surface morphology of samples. The specific surface area tester (SSAT) is used to measure the specific surface area of a sample. The reagents used in the experiment

include anhydrous zinc acetate, anhydrous ethanol, citric acid, sodium hydroxide, methyl orange, granular ZnO, ferric oxide, benzoic acid, benzene, butanol, benzoquinone, ethylenediaminetetraacetic acid, silver nitrate, and deionized water. These reagents play different roles in experiments, such as anhydrous zinc acetate, anhydrous ethanol, and citric acid, which are commonly used in the synthesis and preparation of samples. Sodium hydroxide and methyl orange are used to adjust the pH value of the solution and experimental conditions such as staining. Particles such as ZnO and ferric oxide are used to prepare composite materials and catalysts. Organic solvents such as benzoic acid and benzene are used to dissolve samples and extract active ingredients. Succinol and benzoquinone are used in chemical reactions such as redox reactions. Ethylenediaminetetraacetic acid and silver nitrate are used for experimental operations such as ion exchange and complexation reactions. All reagents have reached the standard of analytical purity, which means they have been highly purified and processed, with high purity and quality. Most of the manufacturers of these reagents are China National Pharmaceutical Group Chemical Reagent Co., Ltd. and Shanghai Lianshi Chemical Reagent Co., Ltd. These two companies are well-known domestic reagent production and sales enterprises, with high popularity and credibility. These reagents played a crucial role in the experiment, ensuring the accuracy and reliability of the experimental results.

3.2 Sample preparation

Hydrothermal method refers to the use of aqueous solution as the reaction system in a specially designed closed reactor. It is an effective method of inorganic synthesis and material treatment by heating and pressurizing the reaction system to create a relatively high temperature and high pressure reaction environment, allowing usually insoluble or insoluble substances to be dissolved and recrystallized. This study used a hydrothermal synthesis method to prepare different N-ZnO, and the obtained N-ZnO was combined with ultrasound to degrade dye wastewater. The sample preparation process is Figure 3.

In Figure 3, the preparation process of snowflake shaped N-ZnO is divided into five steps. The step 1 is to dissolve 0.8 g of $C_4H_6O_4Zn$ and 0.6 g of $C_6H_8O_7$ in 50 mL of ionic water to form a uniform solution. This is achieved by slowly adding $C_4H_6O_4Zn$ and $C_6H_8O_7$ powders to ionic water and continuously stirring. During this process, $C_4H_6O_4Zn$ and $C_6H_8O_7$ are completely dissolved in ionic water, forming a homogeneous and stable solution. Step 2, drop the solu-
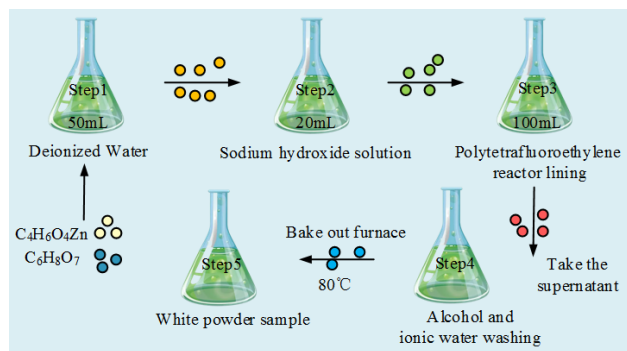
Figure 3. Sample preparation process.

Figure 4. Experimental Steps.

tion prepared in the first step into 20 milliliters of 1 mol/L sodium hydroxide solution and shake for 1 hour under the action of ultrasound. During this process, $C_4H_6O_4Zn$ and $C_6H_8O_7$ react chemically with sodium hydroxide to form ZnO nanocrystals. The function of ultrasound is to promote the reaction and maintain the uniformity and stability of the solution. Step 3, place the solution prepared in step two into a PTFE reactor liner containing 100 milliliters, and then heat the reactor in a 120° C oven for 24 hours. This is to promote the nucleation and growth of ZnO nanocrystals, resulting in ZnO nanomaterials with snowflake like characteristics. The function of the PTFE reactor liner is to provide a uniform thermal field and ensure the progress of the reaction. Step 4, cool the solution prepared in step three to room temperature and remove the supernatant. Wash multiple times with alcohol and deionized water to remove insoluble substances and impurities. This is to remove impurities and insoluble substances in the reaction and obtain pure snowflake like ZnO nanomaterials. Step 5, place the sample prepared in step 4 into an oven, set the temperature to 80° C for baking, and set the drying time to half a day [17–19]. This is to remove moisture and solvents from the sample and obtain dry and stable snowflake like ZnO nanomaterials. After the preparation of N-ZnO is completed, the experiment uses methyl orange to simulate wastewater, and then uses ultrasound technology in conjunction with N-ZnO to treat the simulated wastewater. The degradation results of the simulated dye wastewater are tested using UV visible spectroscopy. The specific experimental steps are shown in Figure 4.

In Figure 4, first weigh 4 mg of methyl orange powder and prepare a 4 mg/L methyl orange solution as a simulation of dye wastewater, which is stored under shading. Add an appropriate amount of N-ZnO to 100 mL of the aforementioned methyl orange solution. Then, put the mixed solution into the ultrasonic device and adjust the device to the desired frequency and temperature. Finally, every 20 minutes, use a pipette to remove 4 mL of the test sample for UV spectroscopy analysis. The specific operation steps of using a UV visible spectrophotometer for analysis and determination in this study are: preheating the UV visible spectrophotometer, selecting the absorption measurement mode, and setting the wavelength range to $200 - 700$ nm. Using the absorbance of ionized water without adding anything as a reference, a total of 6 measurements were
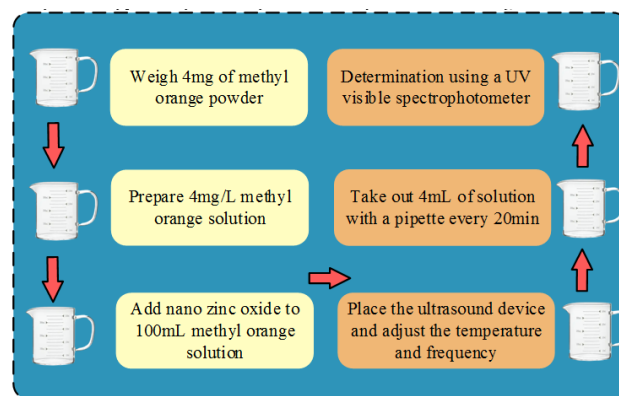
conducted on simulated dye wastewater with a treatment interval of 20 minutes [20]. If the dye concentration is high, the peak values of characteristic peaks in the UV visible spectroscopy will also be relatively large. Given that the characteristic peak of methyl orange solution is around 463 nm, the change in absorbance value at 463 nm can be recorded to deduce the degradation rate of methyl orange at different times. The degradation rate is shown in Equation 1.

$$\text{Degradation rate}(\%) = \frac{H_0 - H_i}{H_0} \times 100\% \qquad (1)$$

In Equation (1), H_0 represents the absorbance value before treatment. H represents the absorbance values at different times after processing.

4. Experimental results

4.1 Analysis of characterization results of N-ZnO materials

The determination of characterization methods is often analyzed and tested using instruments such as X-rPD, SEM, and SSAT. X-rPD is a commonly used phase analysis method that can be used to determine the crystal structure and phase composition of samples. SEM can observe the surface morphology and micro-structure of the sample. SSAT can measure surface properties such as specific surface area of samples. These characterization methods play an important role in experiments, helping researchers gain a deeper understanding of the structure and properties of the samples. The scanning results of spherical N-ZnO, starfish shaped N-ZnO, and snowflake shaped N-ZnO are shown in Figure 5.

In Figure 5, there are significant changes in the appearance characteristics of N-ZnO prepared under different conditions. The red box represents a schematic diagram of three types of nanographic shapes. The nano zinc oxide observed in Figure 5a exhibits a relatively irregular morphology, with uneven size distribution, mainly manifested as a complex structure resembling snowflakes. The size distribution range of these particles is roughly between 100 nanometers and 400 nanometers. This irregularity may be due to the non-uniform growth dynamics during the synthesis process, resulting in the diversity of particle shapes and sizes. This type of structure may have a significant impact on its surface
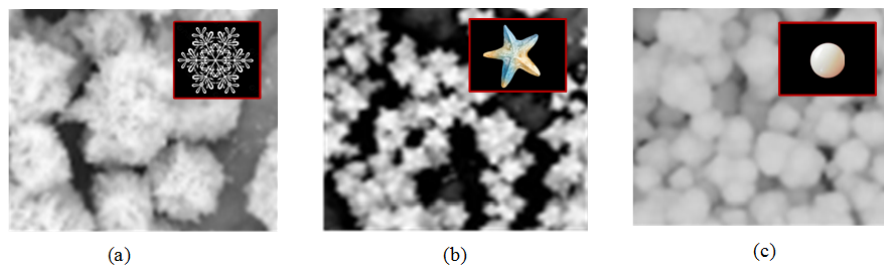
Figure 5. Preparation of zinc oxide scanning images under different conditions. Note: (a), (b), and (c) respectively represent the three forms of N-ZnO.

activity and optical properties. The nano zinc oxide shown in Figure 5b exhibits different morphologies, with a relatively smooth surface and an average particle diameter of approximately 200 nanometers. Compared with the sample in Figure 5a, these nanoparticles are significantly smaller and have an overall morphology similar to starfish. The formation of this structure may be related to the relatively uniform growth environment under synthetic conditions, such as the control of factors such as temperature, pH value, and solvent type. The starfish like structure may promote specific surface reactivity and photocatalytic performance. The nano zinc oxide in Figure 5c exhibits a more regular spherical structure, with a diameter of approximately 100 nanometers, which is the smallest of these three forms. These spherical nanoparticles have a smooth surface and relatively uniform size distribution, which may be due to the strict control of growth conditions and chemical ratios used in the synthesis process. Spherical structures are usually beneficial for improving the dispersion and stability of materials, which is particularly important for catalytic and sensing applications. The X-ray diffraction results of the three types of N-ZnO states are shown in Figure 6.

Figure 6 shows that the diffraction peak effects of three different shaped N-ZnO samples prepared are consistent with the peak values provided on the standard card. This result indicates that all three types of N-ZnO with different shapes have a wurtzite crystal structure. This structure is a common form of ZnO with hexagonal symmetry and has been widely studied and used. At the same time, it was observed that the diffraction peak of N-ZnO exhibited high intensity, and the diffraction peak was sharp, indicating that N-ZnO
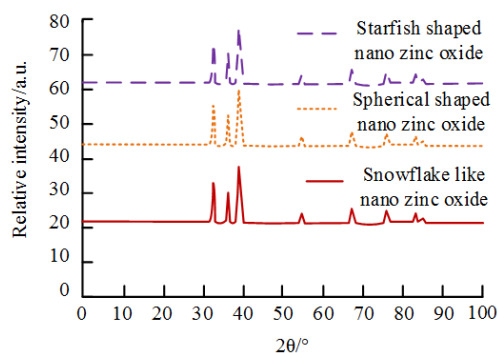
prepared by hydrothermal method has high crystallinity and purity. In addition, the peak curve indicates a narrow half peak width, which is an indicator of good crystallinity of the sample. Furthermore, the absence of impurity peaks further confirms the high purity of the prepared N-ZnO. The N2 adsorption results of the three types of N-ZnO states are shown in Figure 7.

Figure 7 shows the nitrogen adsorption and desorption isotherms of different forms of N-ZnO. There is a hysteresis loop between the adsorption and desorption isotherms of three types of N-ZnO. This phenomenon is usually caused by uneven pore structure or the presence of mesopores. There was no significant saturation adsorption phenomenon observed in the hysteresis loop isotherm. This indicates that the pore structure distribution of these three types of N-ZnO is not uniform. In the case of uneven distribution of pore structure, the specific surface area and pore volume of the material will also be affected, leading to uneven adsorption performance. In addition, the uneven pore structure may also affect the application performance of N-ZnO in gas phase separation, catalyst support, energy storage and release, and other aspects. Therefore, it is crucial to understand the pore structure characteristics and control the pore structure distribution of these N-ZnO with different shapes.

4.2 Comparative analysis of the performance of N-ZnO synergistic ultrasound degradation of dye wastewater

To verify the superiority of the research method in the synergistic degradation of dye wastewater by N-ZnO and ultrasound, this study will compare and analyze the ultrasonic
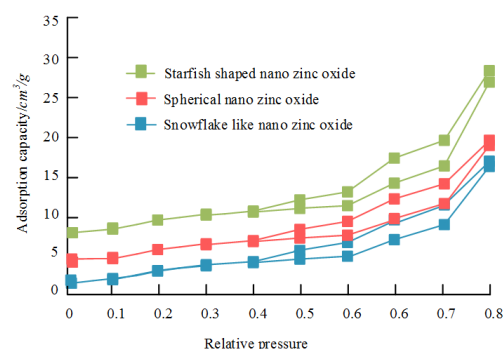

Figure 6. X-ray diffraction patterns of zinc oxide with different morphologies.

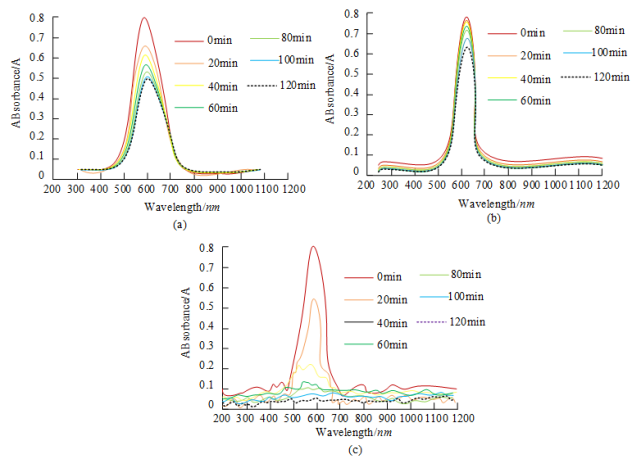**Figure 7.** Adsorption desorption isotherms of N-ZnO with different morphologies.

Figure 8. UV spectrogram of degradation results
Note: (a), (b), and (c) respectively show the UV spectra of ultrasound only, N-ZnO only, and N-ZnO ultrasound synergistic degradation of dye methyl orange solution.

Figure 10. First order kinetic fitting of ultrasound+methyl orange, N-ZnO+methyl orange, and ultrasound+N-ZnO+methyl orange chart.

treatment, N-ZnO treatment, and combined treatment separately. Adjust the ultrasound frequency to 37.00 kHz, power to 20 W, N-ZnO dosage to 100 mg, and reaction time to 2 h. The absorbance results of the three methods are shown in Figure 8.

In the experiment shown in Figure 8a, methyl orange was used as an organic pollutant dye model to evaluate the degradation efficiency of ultrasonic radiation treatment within 2 hours by monitoring its absorbance attenuation at a specific wavelength. The results showed that within the first 20 minutes of ultrasound treatment, the absorption intensity of methyl orange in the solution significantly decreased, indicating that ultrasound can accelerate the degradation process of molecules. However, the absorbance decay rate gradually slowed down, and by 2 hours, the total degradation rate reached 37.50%, indicating the existence of a relatively slow post degradation dynamic. For the data presented in Figure 8b, nano zinc oxide was used as a photocatalyst to independently treat the methyl orange solution. It was observed that the absorbance gradually decreased with time, but the overall degradation efficiency was relatively low, with a 2-hour degradation rate of 18.75%. This indicates that the use of nano zinc oxide alone has limited
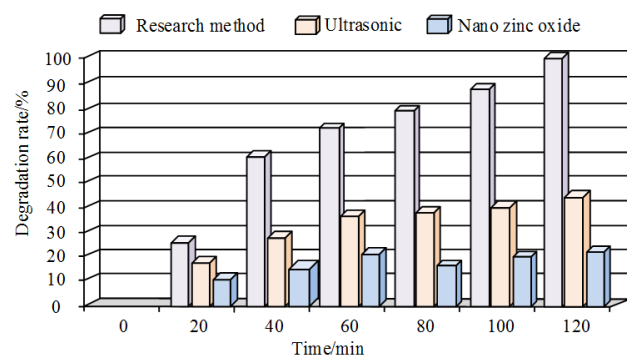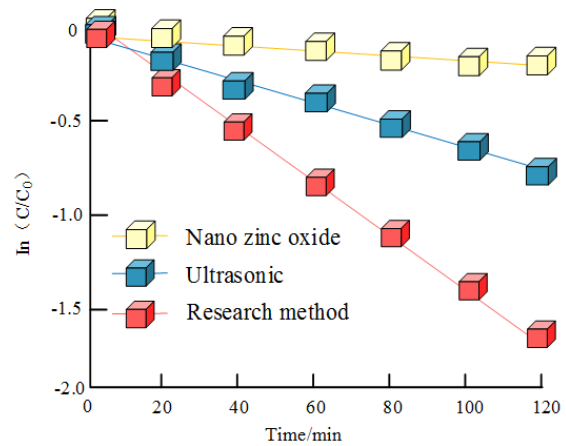
catalytic degradation of pollutants in the absence of other synergistic factors. Further examination of the comprehensive treatment method in Figure 8c shows a significant degradation effect on methyl orange within 2 hours. This method achieved a degradation efficiency of 50.07% within the first 20 minutes, which is significantly faster than the first two methods. As the processing time extended to 2 hours, the absorbance of the solution decreased to 0.012A, significantly lower than other treatment groups. This result indicates that the comprehensive method significantly improves the degradation ability of methyl orange and can efficiently destroy its chromophores, leading to decomposition into small molecules, thereby significantly reducing the visible light absorption capacity of the solution [21–23]. In Figure 9, when only N-ZnO is added, because it is a type of catalyst with adsorption, the dye will be partially degraded, but the degradation effect is poor. When only ultrasound is used for treatment, ultrasound has a cavitation effect, and the generated hydroxyl and free radicals have a certain degradation effect on the dye, with a higher degradation rate than when only N-ZnO is added. When the two are combined for treatment, the degradation rate significantly increases, reaching 99.23% after 2 hours, which is 76.68% higher than the degradation rate using only N-ZnO and 51.52% higher than the degradation rate using only
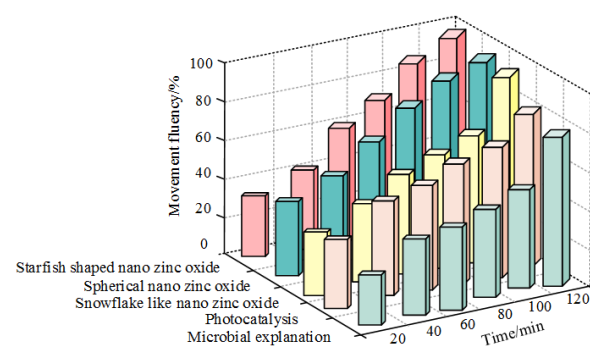

Figure 9. Comparison of degradation effects of ultrasound, nano zinc oxide, and their synergistic effects.

Figure 11. Comparison of degradation effects of nano zinc oxide with different morphologies.

ultrasound treatment. This may be because the synergistic effect of ultrasound and N-ZnO promotes the formation of cavitation bubbles. To further validate the superiority of the research method, the degradation rates of the three methods were compared, as shown in Figure 10.

Based on the Langmuir Hinshelwood model, the first-order dynamic curves of three processing methods were plotted using experimental data in Figure 10, and their k values and correlation coefficients were obtained. Among them, C represents the concentration of Rhodamine, and C_0 represents the initial concentration of Rhodamine. The k-value of the curve with only N-ZnO added is 0.045 min^{-1}, and the R^2 is 0.991. The k value of the curve treated with ultrasound alone is 0.014 min^{-1}, and the R^2 is 0.997. The k-value of the curve processed by combining the two is 0.002 min^{-1}, and the R^2 is 0.995, indicating that the degradation rate of the research method is the highest.

4.3 Comparison of the synergistic ultrasound degradation effect of N-ZnO with different shapes on dye wastewater

To investigate the effect of different shapes of N-ZnO on the synergistic ultrasound degradation of dye wastewater, the most suitable shape was selected and combined with ultrasound for degradation application. This study compares and analyzes the degradation effects of N-ZnO with snowflake, spherical, and starfish shaped shapes combined with ultrasound. Meanwhile, compared with the treatment methods of light treatment (using titanium dioxide as a catalyst) and microbial degradation (white rot fungi), The analysis results are shown in Figure 11.

In Figure 11, before 40 minutes, the degradation rate of spherical and snowflake shaped N-ZnO was faster, while after 50 minutes, the degradation rate of starfish shaped N-ZnO accelerated. After 60 minutes, the degradation rate of starfish shaped N-ZnO was the highest, reaching its maximum value of 99.56% after 2 hours. At 2 hours, the degradation rate of spherical N-ZnO was 98.23%, and the degradation rate of snowflake shaped N-ZnO was 95.23%. Therefore, the degradation effect of starfish shaped N-ZnO is the best, superior to spherical and snowflake shaped N-ZnO. The reason for the inconsistent degradation effects of the three shapes may be the inconsistent size of the specific surface area. The larger the specific surface area, the more points available for reaction, which is more conducive to degradation experiments. Among the three types of N-ZnO, the star shaped N-ZnO has the largest specific surface area. In comparison with the treatment methods of light treatment and microbial degradation, the degradation rate of the two has not yet reached 80% after 2 hours, which verifies the superiority of nano zinc oxide combined with ultrasound treatment of dye wastewater.

5. Conclusion

The study combines nanomaterials with ultrasound technology to explore the synergistic ultrasound degradation performance of different morphologies of nano zinc oxide in dye wastewater, providing new solutions for dye wastewater treatment. In the comparative experiment of

using nano zinc oxide, ultrasound, ultrasound+nano zinc oxide to treat methyl orange solution, the research method showed the most significant change in absorbance, which decreased to the lowest point in a short time. At 20 minutes, the absorbance decreased by 50.07%, and after 2 hours, the absorbance decreased to 0.012A; The research method for treating methyl orange solution significantly improved the degradation rate, reaching 99.23% after 2 hours, which was 76.68% higher than the degradation rate using only nano zinc oxide and 51.52% higher than the degradation rate using only ultrasound treatment. In the comparison between the treatment of three types of nano zinc oxide and the treatment methods of light treatment and microbial degradation, the degradation rate of starfish shaped nano zinc oxide is the highest, reaching the maximum value of 99.56% after 2 hours, which is better than the treatment effect of spherical and snowflake shaped nano zinc oxide, and also significantly better than the treatment methods of light treatment and microbial degradation. The research results validated the applicability and superiority of the research method, and pointed out that starfish shaped nano zinc oxide is most suitable for degrading dye wastewater. However, there are still shortcomings in this study. The experiment only used a single dye for degradation, and the composition of the wastewater is relatively complex. In future research, multiple dyes will be mixed to make it more in line with the actual situation of the wastewater.

References

[1] Z. Wu, Y. Zhao, and N. Zhang. "A literature survey of green and low-carbon economics using natural experiment approaches in top field journal.". *Green and Low-Carbon Economy*, **1**:2–14, 2023. DOI: https://doi.org/10.47852/bonviewGLCE3202827.

[2] F. Hussan, D. Krishna, V. C. Preetam, P. B. Reddy, and S. Gurram. "Dietary supplementation of nano zinc oxide on performance, carcass, serum and meat quality parameters of commercial broilers.". *Biological Trace Element Research*, **200**:348–353, 2022. DOI: https://doi.org/10.1007/s12011-021-02635-z.

[3] A. Rajbhandari Nyachhyon, S. Hajam, and H. M. Trital. "Nano zinc oxide additive for the enhancement of lubricant properties. ". *Scientific World*, **15**:26–32, 2022.

[4] D. Duraibabu, R. Manjumeena, and V. Shalini. "Nano zinc oxide as reinforcing additive to TGDDM epoxy resin for augmented thermo mechanical and antifungal properties.". *Silicon*, **14**:12573–12585, 2022. DOI: https://doi.org/10.1007/s12633-022-01966-3.

[5] D. Solomon, Z. Kiflie, and S. Van Hulle. "Using Box–Behnken experimental design to optimize the degradation of Basic Blue 41 dye by Fenton reaction.". *International Journal of Industrial Chemistry*, **11**:43–53, 2020. DOI: https://doi.org/10.1007/s40090-020-00201-5.

[6] A Zamani, M. S. Sadjadi, A. Mahjoub, M. Yousefi, and N. Farhadyar. "Synthesis, characterization and investigation of photocatalytic activity of ZnMnO3/Fe3 O4 nanocomposite for degradation of dye Congo red under visible light irradiation.". *International Journal of Industrial Chemistry*, **11**:205–216, 2020. DOI: https://doi.org/10.1007/s40090-020-00215-z.

[7] S. Kh. Al-Taee and A. H. Alhamdani. "Quantification histopathological analysis in the gills of carp fish exposed to sub lethal concentration of nano zinc oxide. ". *Iraqi Journal of Veterinary Sciences*, **36(Supplement I)**:61–68, 2022. DOI: https://doi.org/10.33899/ijvs.2022.135365.2471.

[8] A. N. Taha and H. Kh. Ismail. "The impact of nano zinc oxide particles on the histology of the male reproductive system of adult male rabbits.". *Iraqi Journal of Veterinary Sciences*, **37**:105–113, 2022. DOI: https://doi.org/10.33899/IJVS.2022.133632.2270.

[9] S. K. John and S. G. Benjamin. "In situ precipitation and characterization of nano zinc oxide in different polymeric media and photoluminescent properties.". *Research Journal of Chemistry and Environment*, **27**: 39–47, 2023.

[10] R. Assim Hameed. "Effectiveness of phenol compound isolated from menthe spicata leaves and nano-zinc oxide on antimicrobial activity.". *Al-Kufa University Journal for Biology*, **15**:18–26, 2023. DOI: https://doi.org/10.36320/ajb/v15.i1.11723.

[11] F. C. Chen, C. M. Huang, and X. W. Yu. "Effect of nano zinc oxide on proliferation and toxicity of human gingival cells.". *Human & Experimental Toxicology*, **40**:804–813, 2022. DOI: https://doi.org/10.1177/09603271221080237.

[12] M. Hong, J. L. Gong, W. C. Cao, R. Fang, Z. Cai, J. Ye, Z-P. Chen, and W-W. Tang. "The combined toxicity and mechanism of multi-walled carbon nanotubes and nano zinc oxide toward the cabbage.". *Environmental Science and Pollution Research*, **29**:3540–3554, 2022. DOI: https://doi.org/10.1007/s11356-021-15857-4.

[13] N. Pruthvi Raj and C. P. Chandrashekara. " Impact of nano zinc oxide application on quality parameters of Bt cotton (Gossypium hirsutum L.).". *International Journal of Chemical Studies*, **9**:153–158, 2021. DOI: https://doi.org/10.22271/chemi.2021.v9.i2b.11939.

[14] B. Al-Mistarehi, A. Al-Omari, M. Taamneh, R. Imam, and D. Khafaja. "The effects of adding Nano Clay and Nano Zinc Oxide on asphalt cement rheology. ". *Journal of King Saud University - Engineering Sciences*, **35**:260–269, 2023. DOI: https://doi.org/10.1016/j.jksues.2021.03.010.

[15] S. Yuan, F. Yang, and H. Yu. "Ultrasonic stimulation of milk fermentation: effects on degradation of pesticides and physiochemical, antioxidant, and flavor properties of yogurt.". *Journal of the Science of Food and Agriculture*, **102**:6612–6622, 2022. DOI: https://doi.org/10.1002/jsfa.12028.

[16] S. X. Gan, C. Jia, and Q. Y. Qi. "A facile and scale-up synthetic method for covalent organic nanosheets: ultrasonic polycondensation and photocatalytic degradation of organic pollutants. ". *Chemical Science*, **13**:1009–1015, 2021. DOI: https://doi.org/10.1039/D1SC05504F.

[17] M. M. Aung, W. J. Li, and H. N. Lim. "Improvement of anticorrosion coating properties in bio-based polymer epoxy acrylate incorporated with nano zinc oxide particles.". *Industrial Engineering Chemistry Research*, **59**:1753–1763, 2020. DOI: https://doi.org/10.1021/acs.iecr.9b05639.

[18] A. K. Gupta, R. K. Samaiya, and Y. Singh. "Effect of nano zinc oxide seed treatment on physiological growth and biophysical traits and seed quality of soybean [Glycine max (L.) Merrill]. ". *International Journal of Environment and Climate Change*, **13**:687–699, 2023. DOI: https://doi.org/10.9734/ijecc/2023/v13i71921.

[19] S. Mahdavi, R. Karimi, and A. Valipouri Goudarzi. "Effect of nano zinc oxide, nano zinc chelate and zinc sulfate on vineyard soil Zn- availability and grapevines (Vitis vinifera L.) yield and quality.". . *Journal of Plant Nutrition*, **45**:1961–1976, 2022. DOI: https://doi.org/10.1080/01904167.2022.2046081.

[20] S. Ahmadi, C. A. Igwegbe, and S. Rahdar. "The application of thermally activated persulfate for degradation of Acid Blue 92 in aqueous solution. ". *International Journal of Industrial Chemistry*, **10**:249–260, 2019. DOI: https://doi.org/10.1007/s40090-019-0188-1.

[21] A. Tarafdar, O. Razmkhah, and H. Ahmadi. "Effect of layering layout on the energy absorbance of bamboo-inspired tubular composites.". *Journal of Reinforced Plastics and Composites*, **41**:602–623, 2022. DOI: https://doi.org/10.1177/07316844211063865.

[22] A. Lace, A. Byrne, and S. Bluett. "Ion chromatograph with three-dimensional printed absorbance detector for indirect ultraviolet absorbance detection of phosphate in effluent and natural waters.". *Journal of Separation Science*, **45**:1042–1050, 2022. DOI: https://doi.org/10.1002/jssc.202100897.

[23] J. Tienaho, N. Silvan, and R. Muilu-Mäkelä. "Ultraviolet absorbance of Sphagnum magellanicum, S. fallax and S. fuscum extracts with seasonal and species-specific variation.". *Photochemical & Photobiological Sciences*, **20**:379–389, 2021. DOI: https://doi.org/10.1007/s43630-021-00026-w.